RESEARCH ARTICLE

Study of physical and mechanical properties of BG/HA/TiO$_2$ biocomposite for bone implantation.

*Sunil Prasad[1], Vikas Kumar Vyas[1], Kumari Deepa Mani[2], Ram Pyare[1].
1. Department of Ceramic Engineering, Indian Institute of Technology (BHU), Varanasi-221005, India.
2. Department of Zoology, BHU, Varanasi-221005, India.

Manuscript Info

Abstract

In the present study composition of HA, TiO$_2$ and bioglass were successfully synthesized and biocomposites were prepared by powder metallurgy method. Microstructure and morphology of the biocomposites were examined by scanning electron microscopy (SEM). Analytical, thermal and microstructural investigations were carried out by XRD, SEM, DTA/TGA techniques, and results shows considerable higher rates of apatite formations. The dissolution behavior of the bioactive glasses and biocomposites in SBF showed in vitro test for all samples. Addition of X%HA and X%TiO$_2$ in (100-2X%) 45S5 bioglass improves mechanical properties such as hardness, compressive strength, elastic modulus of these biocomposites.

Introduction:-

The first bioactive glass was made by Hench which was known as (45S5) Bioglasss (A. Huygh et al.,2002). Bioactive glasses belong to an influential class of biomaterials which are generally based on amorphous silicate compounds (E. Schepers et al.,1991). The author made a degradable glass in the Na$_2$O–CaO–SiO$_2$–P$_2$O$_5$ system which was rich in CaO content and the composition of this was close to a ternary Na$_2$O–CaO–SiO$_2$ system (Julian R. Jones et al.,2013; L.L. and Hench et al.,2006). It is well known that these materials are able to bind with the bones in living organisms and have been clinically used in dental and orthopedic implantation (L.L. Hench et al.,1971). HCA is similar to bone mineral and was believed to interact with collagen fibrils which bonds with the host bone. The osteogenic properties of the glass were considered to be due to the dissolution types of the glass (L.L. Hench et al.,2002). This paper reviewed and discuss current knowledge on porous bone tissue engineering scaffolds on the basis of melt-derived bioactive silicate glass compositions and relevant composite structures (Lutz-Christian Gerhardt et al.,2010).

Hydroxyapatite (HA, Ca$_{10}$(PO$_4$)$_6$(OH)$_2$) has the ability to form strong chemical bonds with natural bone because of its similar chemical and crystallographic structure like the apatite of living bone. But one of its primary restrictions in clinical use is load-bearing implants because it has poor mechanical property (C. Q. Ning et al.,2000 and K. DE Groot et al.,1980). Our study with the SiO$_2$–CaO–P$_2$O$_5$–K$_2$O–Al$_2$O$_3$ based bioactive glasses suggests that the material could be used in bone replacement for clinical cases. The bioactive glasses have demonstrated high degree of tolerance for the RBC and WBC which strongly supports its suitability as an alternative for bone replacement (Himanshu Tripathi et al.,2015). Hydroxyapatite (Ca$_{10}$(PO$_4$)$_6$(OH)$_2$, HA) has been attracting much attention as a material for artificial bones (Hench LL et al.,1998) and scaffolds for tissue engineering. Hydroxyapatite has been widely used as a bone substitute material in restorative dental and orthopedic implants, due to its chemical and crystallographic structure being similar to that of bone mineral [Hench LL et al.,1998; Ebaretonbofa E et al.,2002; Elliott JC et al.,1973; De Groot K et al.,1990; Jarcho M et al.,1981; Ruys AJ et al.,1995].

Experimental:-
2.1 material and methods:-
2.1.1 Preparation of Bioglass:-
Bioglass (45S5) with the chemical compositions 45%SiO_2, 24.5%CaO, 24.5%Na_2O and 6%P_2O_5 in (wt%) was prepared from reagent grade chemicals. Chemicals were weighout, properly mixed and melted in 100 ml platinum crucible at 1400$\pm$5$^{°}$C with air as furnace atmosphere for 4 hours. Melted glasses were poured in water to prepare frit and it was milled to a powder form in a porcelain ball mill for 24 h.

2.1.2 Production of HA:-
In the present study, calcium nitrate tetrahydrate ($Ca(NO_3)_2 \cdot 4H_2O$) (CNT) (G.S. Chemical Testing Lab. & allied industries,India), phosphoric acid (H_3PO_4)(Loba Chemie Pvt. Ltd, India) and ammonia (NH_3) (Loba Chemie Pvt. Ltd, India)) were used as initial precursors. The schematic presentation of the procedure (K P Santosh et al.,2009) is given in Fig.1.

2.1.3 Preparation of BG/HA/TiO_2 composites:-
The HA and TiO_2 powder were mixed (5, 10, 15 and 20 wt%) with bioglass (45S5) powder, compacted at 1500 MPa pressure into cylindrical samples (1 cm,1 cm) and were sintered at 1150$^{°}$C to prepare the composites as shown in Table 1.

Table 1: Composition of Bioactive glass and Bio-composite (BGHATi1, BGHATi2, BGHATi3, BGHATi4)

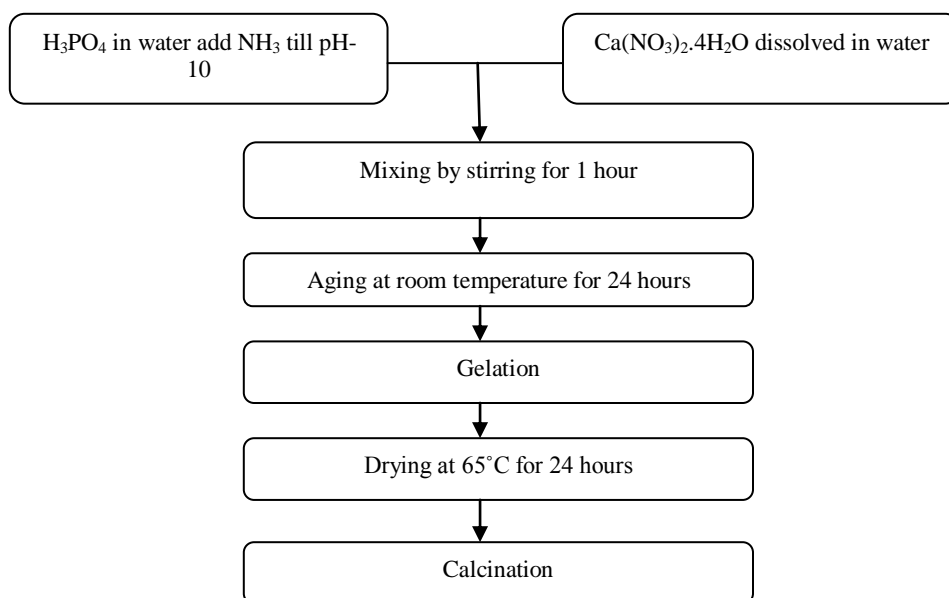| Bio-composite Samples	Composition (wt %)		
	BG (45S5)	HA	TiO_2
BGHATi1	90	05	05
BGHATi2	80	10	10
BGHATi3	70	15	15
BGHATi4	60	20	20

Fig. 1. Flow chart of hydroxyapatite preparation by the sol-gel route.

2.2 Preparation of SBF:-
Kokubo and his colleagues developed simulated body fluid that has an inorganic ion concentrations similar to those of human body fluid in order to reproduce in vitro formation of apatite on bioactive materials (Kokubo T et al.,2006). The SBF solution was prepared by dissolving reagent-grade NaCl, KCl, $NaHCO_3$, $MgCl_2.6H_2O$, $CaCl_2$ and KH_2PO_4 into double distilled water and it was buffered at pH=7.4 with TRIS (trishydroxymethyl amino methane) and 1N HCl at 37$^{°}$C as compared to the human blood plasma (WBC). The ion concentrations of SBF are given in the Table 2 (A. Agarwal et al.,1997).

Table 2: Ion concentration (mM/litre) of simulated body fluid and human blood plasma

	Na^+	K^+	Ca^{2+}	Mg^{2+}	HCO_3^-	Cl^-	HPO_4^{2-}	SO_4^{2-}
Simulated Body Fluid	142.0	5.0	2.5	1.5	4.2	148.0	1.0	0.5
Blood plasma	142.0	5.0	2.5	1.5	27.0	103.0	1.0	0.5

2.3 Physical Analysis:-
Differential thermal analysis (DTA) was carried out on bioactive glass samples which were examined at the temperature of 250°C to 900°C, using alumina as a reference material and the heating rate was 10°C/min. Identification of the crystalline phases after heat treatment of biocomposite samples was carried out by X - ray diffraction (XRD) analysis, adopting Ni filter and Cu target with voltage of 40 KV and a current of 25 mA.

2.4 Powder X-ray diffraction (XRD) measurements:-
The biocomposite samples were ground to 75 microns and the fine powders were subjected to X-ray diffraction analysis (XRD) with RIGAKU-Miniflex II diffractometer adopted Cu-Kα radiation (λ = 1.5405A°) with a tube voltage of 40 kV and current of 35mA in a 2θ range between 20° and 80°. The step size and measuring speed was set to $0.02°$ and $1°$ per min respectively, in the present investigation. The JCPDS-International Centre for Diffraction Data Cards were used as a reference.

2.5 Density and Mechanical Properties Measurements:-
Archimedes principle was applied to obtain the density of biocomposite samples using distilled water as buoyant. All the weight measurements were taken using a digital balance (Sartorius,Model: BP221S, USA) having an accuracy of ± 0.0001 g. Density (ρ) of sample was obtained by employing the relation (1) as given below:
$$\rho = \frac{Wa}{Wa - Wb}\rho b \qquad \text{------- (1)}$$
where W_a is the weight of sample in air, W_b is the weight of sample in buoyant and ρb is the density of buoyant. Micro indentations were made on the polished surfaces of bioactive glass composite using a diamond Vickers indenter of a micro hardness testing machine (Future - Tech Corp, Tokyo, Model FM - 7e, Japan). The size of the specimen was 20 mm x 20 mm x 20 mm according to ASTM Standard: C730 - 98. The indentations have been made for loads ranging between 30 mN and 2000 mN, applied at a velocity of 1 mm/s and allowed to equilibrate for 15 seconds before measurement. Microhardness (H) (GPa) of specimen is calculated using the formula (2) as given below:
$$H_v = 1.854\frac{P}{D2} \qquad \text{------ (2)}$$
Where H_v hardness value, P (N) applied load on specimen and D (m) is the diagonal of the impression.

2.5.1 Mechanical behaviour measurements:-
Pellets were prepared by hydraulic press machine in the form of rectangular shape pellets and the resultant biocomposite samples were sintered at 1150°C and polished for required dimension using grinding machine. Samples were subjected to three-point bending test. The test was performed at room temperature using Instron Universal Testing Machine (AGS 10kND, SHIMADZU) of cross-head speed of 0.5 (mm/ min) and full scale load of 2500 kg. Flexural strength was determined according to ASTM Standard: C158 02(2012). Polished bioactive glass samples were subjected to hardness testing machine, size of sample was $10 \times 10 \times 10$ mm according to the ASTM Standard: C730-98. The indentations have been made for loads ranging between 30 and 2000 mN, applied at a velocity of 1(mm/s) and allowed to equilibrate for 16 s before measurement. The densities of casted biocomposites were measured by the Archimedes principle with water as the immersion fluid. The measurements were taken at room temperature. Thin copper wire was used for immersing the samples into water. The density was determined by using ASTM: B962-14. Compressive strength of the biocomposite samples having size of $3\times2\times1$ cm^{-1} dimension according to ASTM D3171 were subjected to compression test. The test was performed using Instron Universal Testing Machine at room temperature (cross speed of 0.05 cm min^{-1} and full scale of 5000 kgf).

2.5.2 Elastic Properties Meassurement:-
The ultrasonic velocities (longitudinal and shear) were measured for HA and TiO_2 reinforcement bioactive glass biocomposites at 5 MHz using the cross correlation technique employing the pulse echo method. A high power Ultrasonic Pulser Receiver Olympus instrument (M-45,USA) manufactured by USA and a digital storage oscilloscope (DSO) (Lecroy, Wave Runner 104 MXi 1GHz, USA) were used for recording ultrasonic (rf) signals.

The precise transit time t was measured employing the cross-correlation technique. Biocomposite samples were cut and polished in cubic pieces and the couplant glycerin was used for finding longitudinal velocities and sonfech shear gel for the shear velocities of biocomposites.

Young's modulus, Shear modulus, Bulk modulus of elasticity and Poisson's ratio were determined by using following formula.

Young's modulus   (E)   = $[V_L^2 \rho (1+v) (1-2v)] / (1-v)$ --------------(3)

Shear modulus   (G)   = $V_T^2 \rho$ --------------(4)

Bulk modulus   (K)   = $E / 3(1-2v)$ -------------(5)

Poisson's ratio   (v)   = $[1-2(V_T/V_L)^2] / [2-2(V_T/V_L)^2]$ ----------------(6)

Results:-
3.1 Physical Analysis:-
3.1.1 Differential Thermal Analysis (DTA):-
The DTA traces of biocomposites show that the incorporation of HA and TiO_2 in the base bioactive glass (45S5) causes a decrease in its endothermic peak temperature as well as its exothermic peak temperature. In the differential thermal analysis (DTA) traces of bioactive glasses (Fig.2), endothermic peak shows the nucleation region and the exothermic peak corresponding to the crystallisation process. Previous studies (E.M.A. Khalil et al.,2010) have shown that in silicate glasses, the presence of transition metal ion's of low doping percentage is not expected to form separate structural units.

TGA curve of biocomposites precursor after drying at 200-900˚C for 4 hr. Three main stages of TGA curve of TiO_2 sample according to the heat profile were observed. The temperature increases from 200 to 240˚C as first stage. In the range of temperature of 250 to 260˚C, is attributed to decomposition of the organic compounds completely with about 8.0 % weight was lost (J. Wang et al.,2008). The amorphous precursor was converted to anatase phase as the temperature increases from 270 to 280˚C. The TiO_2 anatase was transferred to rutile phase between 720 to 740˚C(X. Sun et al.,2010).
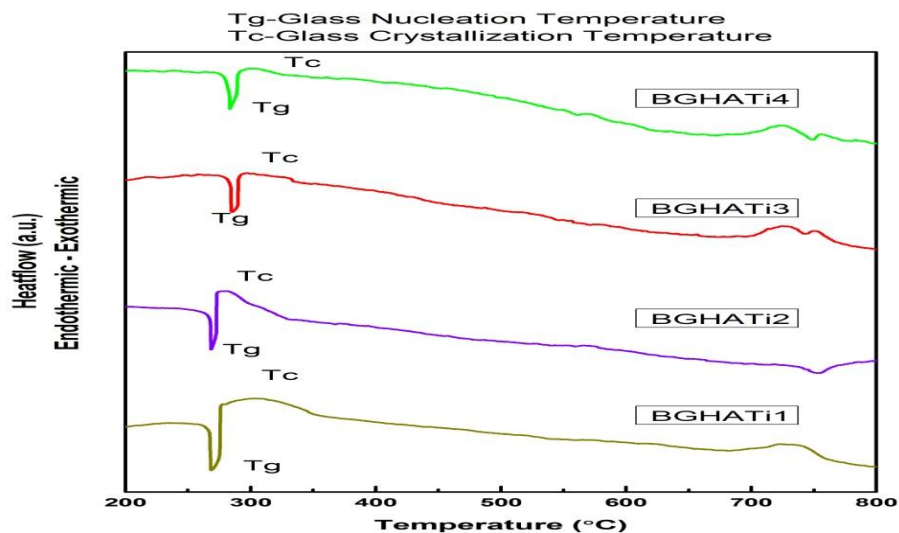

Fig.2. DTA/TGA traces of biocomposite.

3.1.2 Phase analysis:-
The prepared biocomposite samples are BGHATi1, BGHATi2, BGHATi3 and BGHATi4 (all of the samples in Table 1) were characterized by XRD. X-ray powder diffraction data of the prepared biocomposites are shown in Fig.3. The patterns of BGHATi1 composite having high % of BG content do not show any peaks for BG due to its amorphous nature. Intensity of titania peaks is very weak denoting lower content of titania in the BGHATi1 composite. These peaks are recorded at d (A°) = 3.24, 2.99 and 2.61 forming calcium titanium silicate [CaTi(SiO₅)] compound (Card No.: 73-2066) and proving interaction between TiO_2 and BG powders. Fig.3 shows the increase of the intensity of calcium titanium silicate oxide peaks denoting more reaction found between the BG and TiO_2 (Long M et al.,1998) as well as the appearance of some peaks of titania (rutile form) at d (A°) = 2.49, 2.18, 2.06, 1.68 and 1.62 (Card No.: 04-0551) as a result of the conversion of anatase to rutile form which do not react with BG powder.

In this domain, anatase transforms into rutile form at any temperature between 600 and 1000°C (Nanci A et al.,1998). For BGHATi3 composite, Fig. 1 shows the increase of intensity of $CaTi(SiO_5)/TiO_2$ peak at d (A°) = 3.25 with disappearance of the peaks at d (A°) = 2.99.

The peaks of rutile increases and became almost four times compared to those of BGHATi4 composite as a result of the highest titania content in the BG/titania composite proving the presence of part of titania powder which does not react with BG powder and converts completely to the rutile form.

This results show possible reactions during transformation at temperature from 1000 to 1200°C as follows (Albrektsson T et al.,1986)
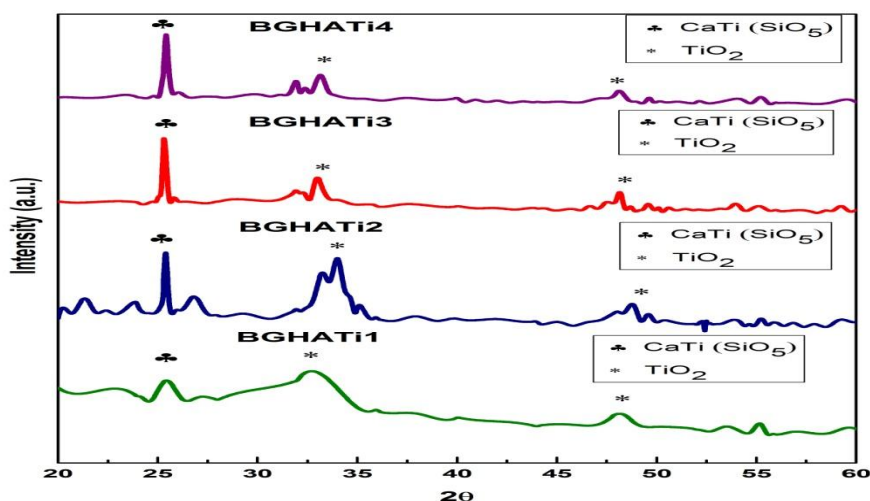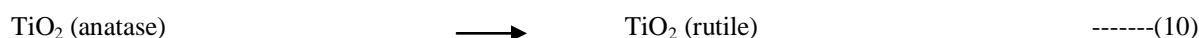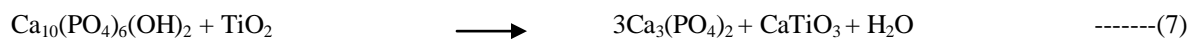
$$Ca_{10}(PO_4)_6(OH)_2 + TiO_2 \longrightarrow 3Ca_3(PO_4)_2 + CaTiO_3 + H_2O \qquad \text{-------(7)}$$

$$Ca_{10}(PO_4)_6(OH)_2 + SiO_2 + TiO_2 \longrightarrow 3Ca_3(PO_4)_2 + CaTiSiO_3 + H_2O \qquad \text{------(8)}$$

$$Ca_8(PO_4)_6 (PO_2OH) + 3/2 Na_2O \longrightarrow Ca_3(PO_4)_2 + Na_2Ca_6(PO_4)_5 + 1/2H_2O + O_2 \qquad \text{--(9)}$$

$$TiO_2 \text{ (anatase)} \longrightarrow TiO_2 \text{ (rutile)} \qquad \text{-------(10)}$$

Fig.3. X-ray diffraction of the prepared BG/HA/TiO_2 composites.

3.1.3 Surface morphology:-

Post-immersion in SBF the glass releases Ca^{2+} and Na^+ ions from its surface via an exchange with the H_3O^+ ion in the SBF to form Si–OH or Ti–OH groups on their surfaces (A.J. Salinas et al.,2002). Water molecules in the SBF simultaneously react with the Si–O–Si or Ti–O–Ti bond to form additional Si–OH or Ti–OH groups, the formed Si–OH and Ti–OH groups induce apatite nucleation, and the released Ca^{2+} and Na^+ ions accelerate apatite nucleation by increasing the ionic activity product of apatite in the fluid (P.N. De Aza et al.,2004). As a result, the apatite layer forms onto the composite surface after soaking in SBF in a short period (3days) and this phenomenon is confirmed by SEM of BG/HA/titania composites post-immersion as shown in Fig.5(a-d). BGHATi1 biocomposites, shows that this composite has many particles on its surface proving slight formation of apatite layer due to the composite contains high content of silica characterizing melted and dense structure that reduced nucleation of apatite layer compared to other composites. In this domain, the simultaneous dissolution of silicates results in the formation of silanol groups on material's surface, which are essential for nucleation sites resulting in HA formation (C. Sarmento et al.,2004). Once the apatite nuclei formed, they can grow spontaneously by consuming the calcium phosphate ions in the surrounding fluid (P.N. De Aza et al.,2000).

For BGHATi2,BGHATi3 and BGHATi4 composites, SEM at the same magnification indicates the presence of rich spherical shapes build up on each other to form a bone-like apatite layer for both composites especially BGHATi4 composites. This result is due to BGHATi4 composites contains high content of titania which leads to increase of

Ti–OH groups at the expense of Si–OH groups resulting in high nucleation of apatite (Fig. 5d). In this study, it was observed that the rutile form of titania is the main phase in four composites and is essential for improvement of apatite nucleation especially BGHATi3 and BGHATi4 composites compared to BGHATi1 composites containing low content of titania. The catalytic effect of the Si–OH groups and Ti–OH groups for the apatite nucleation has proven by the observation that silica and titanium will form apatite on their surfaces in SBF and are abundant on the composite surfaces (C. Sarmento et al.,2004; P.N. De Aza et al.,2000 and P.N. De Aza et al.,1999).
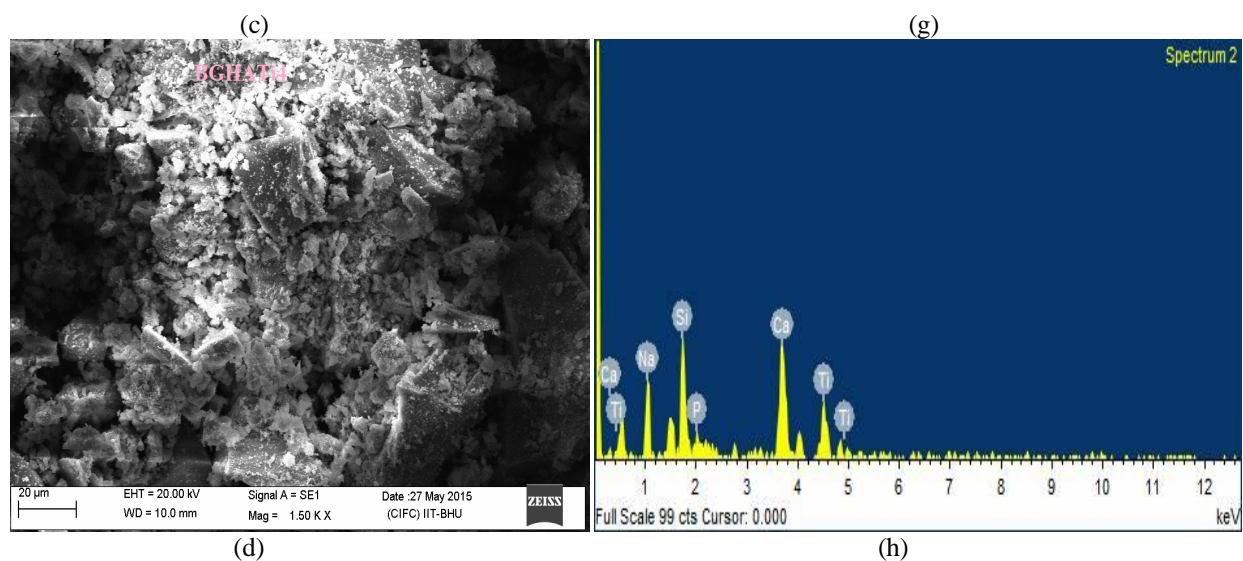

(a)

(e)

(b)

(f)

(c)

273
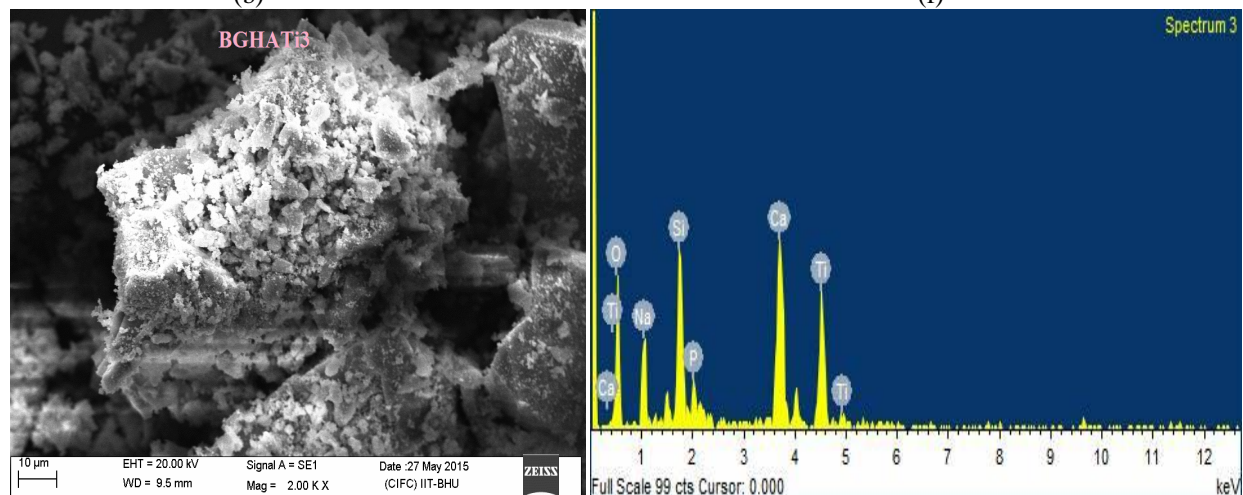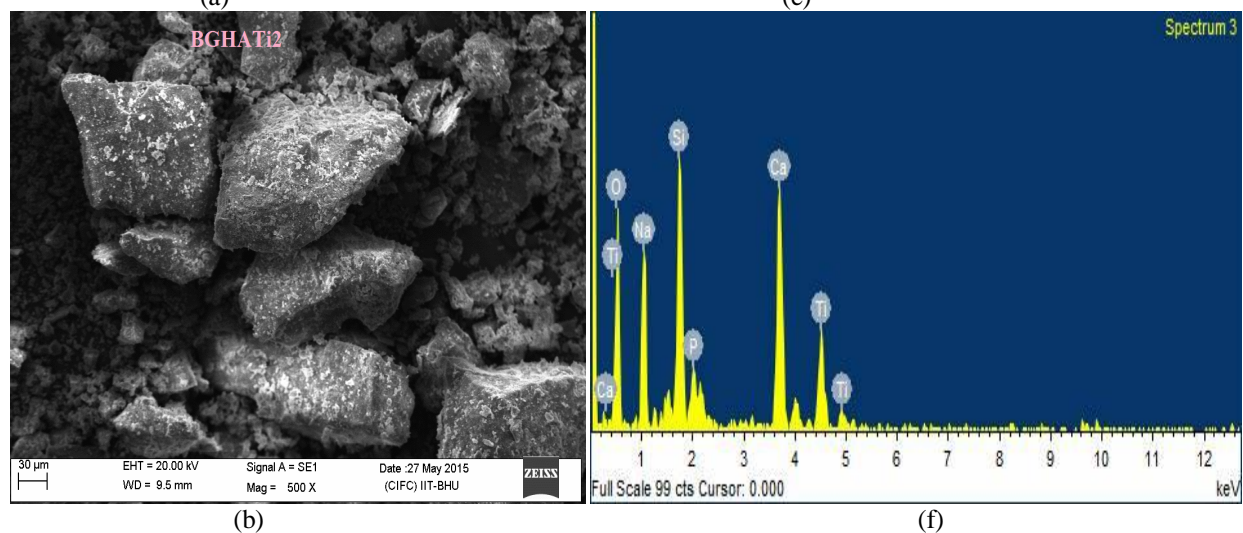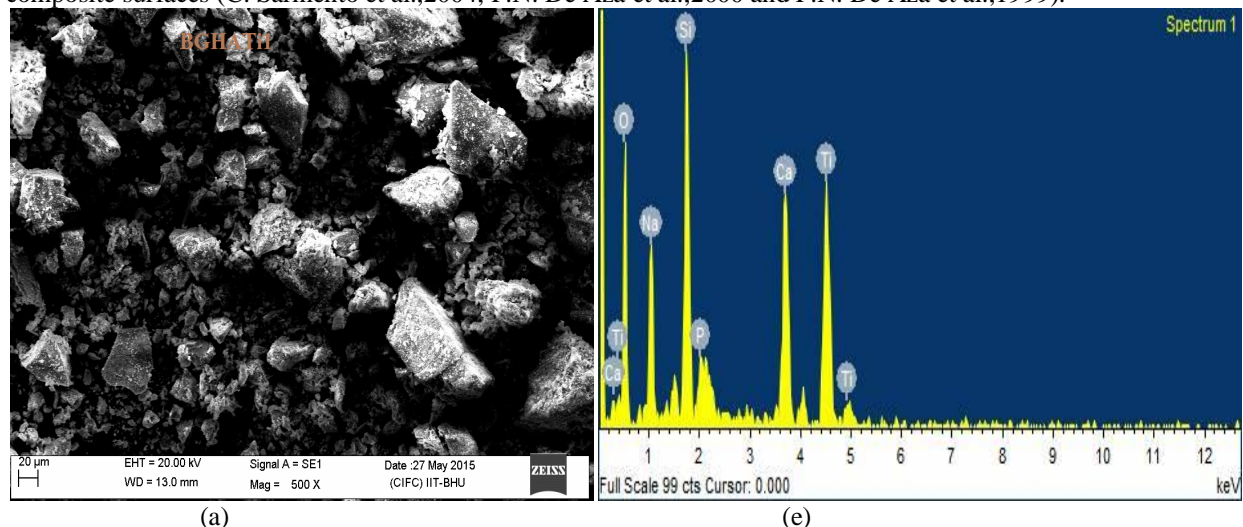
Fig.4   SEM (a-d) and EDAX (e-h) of the BG/HA/TiO$_2$ composites for BGHATi1, BGHATi2, BGHATi3 and BGHATi4 composites post-immersion in SBF.

EDAX point analyses show that Ca, P, and Ti coexist in different properties of sintered pellet as shown in Fig. 4 (e-h) conferming the interfusion between HA and TiO$_2$ particles before their impinging into the substrate.

3.2 pH behavior in SBF:-

The variation in pH values of simulated body fluid (SBF) after soaking of biocomposite for various time periods is shown in Fig. 6. It was observed that the pH of all samples showed the similar tendency of behavior (M.A. Lopes et al.,1998). The maximum pH values was recorded on 1 day of immersion. The change of pH of SBF solution can be explained by ion exchange process on the glass surface. Cations such as Na$^+$ or Ca^{2+} near the glass surface go into solution by exchange of H$^+$ or H$_3$O$^+$ ions from the solutions which results in a pH increase, after certain point decrease in pH can be explained by considering the precipitation of calcium phosphates and carbonates. The update of carbonate and phosphate ions shifts the equilibriums towards the products side, thus causing a decrease in the pH (F. Moztarzadeh et al.,1988). It was observed that addition of HA in base bioactive glass (45S5), sequence of reactions occurred in SBF after immersion of biocomposite for various time periods are in favour of formation of hydroxyapatite layer on the surface of the samples (Marta Cerrutia et al.,2005 and Delia S. Brauer et al.,2010).
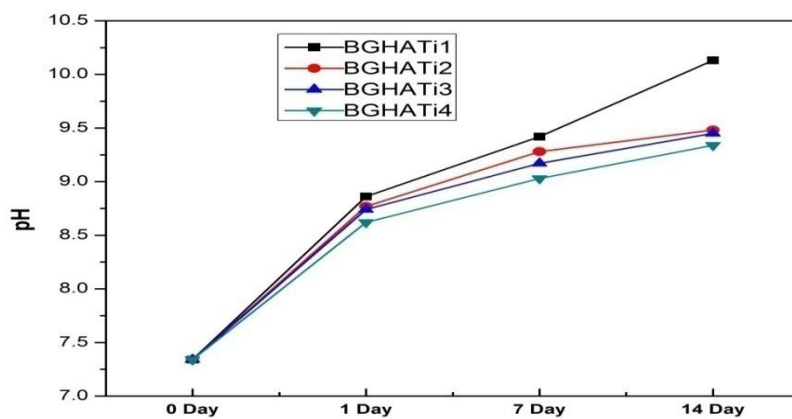
$$HCO_3^{3-} \longrightarrow CO_3^{2-} + H^+ \quad and \quad HPO_4^{2-} \longrightarrow PO_4^{3-} + H^+ \qquad \text{-----------(7)}$$

Fig. 5. pH of different biocomposites (BGHATi1,BGHATi2,BGHATi3,BGHATi4).

3.3 Mechanical Properties:-
3.3.1 Density, Compressive Strength and Hardness of biocomposites:-
The density increased rapidly when the pellet samples were sintered at 1150˚C and 1250˚C due to the partial HA decomposition into α-TCP and TTCP. Density of biocomposite sintered at 1150˚C increased with increasing HA and TiO_2 content as shown in Fig.6 because density of titanium is more than 45S5 bioglass and HA.

Table 3: Density (ρ), longitudinal velocity (V_L) and transverse velocity (V_T), Young's modulus, Shear modulus, Bulk modulus and Poisson's ratio of biocomposites.

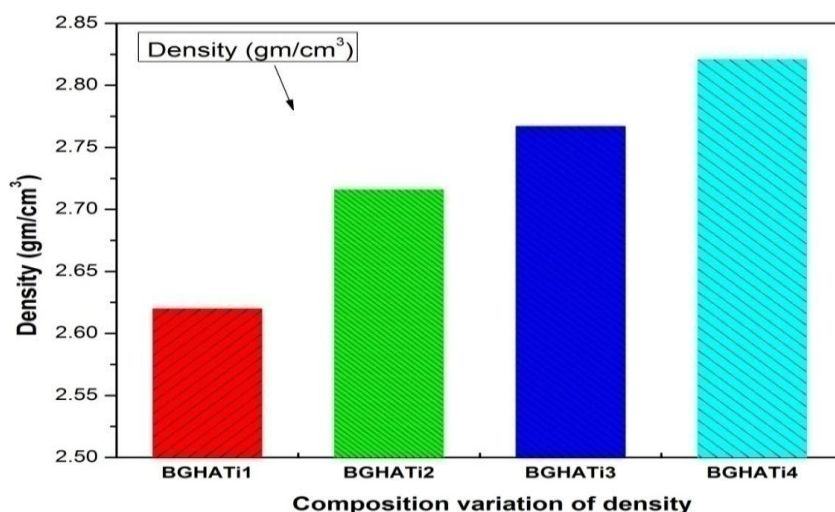| Sample	Density (ρ) (gm/cm^3)	V_L(m/s)	V_T(m/s)	Young's modulus E(GPa)	Shear modulus G(GPa)	Bulk modulus K(GPa)	Poisson's ratio (v)
BGHATi1	2.62	5489	3114	47	25	33	0.2627
BGHATi2	2.72	5605	3210	52	28	35	0.2559
BGHATi3	2.77	5716	3312	75	30	49	0.2472
BGHATi4	2.82	5886	3422	82	33	53	0.2447

Fig.6 Variations of density in different HA and titania reinforced with bioglass composites.

Variation of compressive strength depending on reinforcement content and sintering temperature has shown in Fig.7. The figure shows that increasing reinforcement content from (5, 10, 15 and 20) wt.% increased the compressive strength from 41 to 104 MPa for sintering at 1150˚C. Such a phenomenon can be attributed to the occurrence of a new phase among bioglass, HA and TiO_2 for higher sintering temperatures.
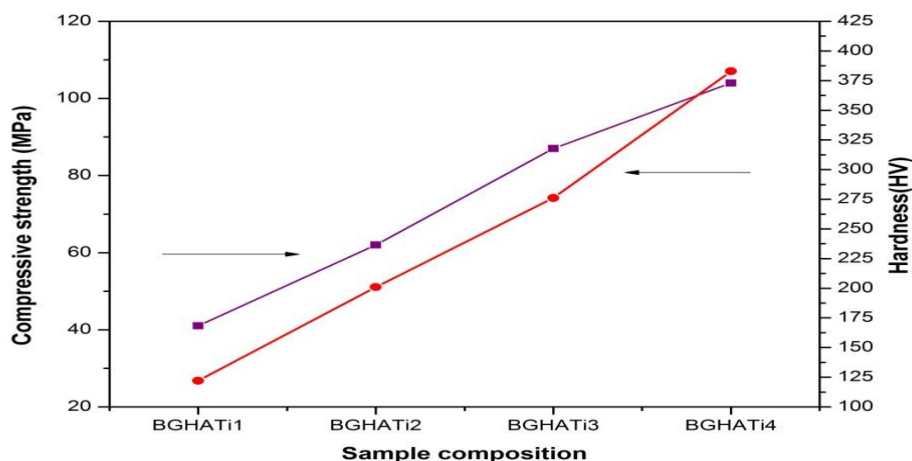
Fig.7 Variation of compressive strength depending on reinforcement content of pellet samples.

3.3.2 Degradation of compressive strength of biocomposite during in vitro test:-

The compressive strength and elastic modulus of the scaffolds after immersion in SBF in vitro are shown in Fig.8(a) as a function of immersion time or implantation time. The strength and modulus decreased rapidly during first 3 weeks but more slowly thereafter. This trend was independent of the in vitro environment. The strength decreased from the as fabricated value of 104±8MPa to 84±5MPa after 3 weeks in SBF in vitro test. After 12 weeks, the strength of the scaffolds immersed in SBF was 73±8MPa. The elastic modulus of the scaffolds decreased from the as fabricated value of 82±8GPa to 75±5GPa after 3 weeks in SBF in vitro Fig.8(b). The modulus of the scaffolds was 66±8GPa, respectively after 12 weeks in SBF and in vitro environment.
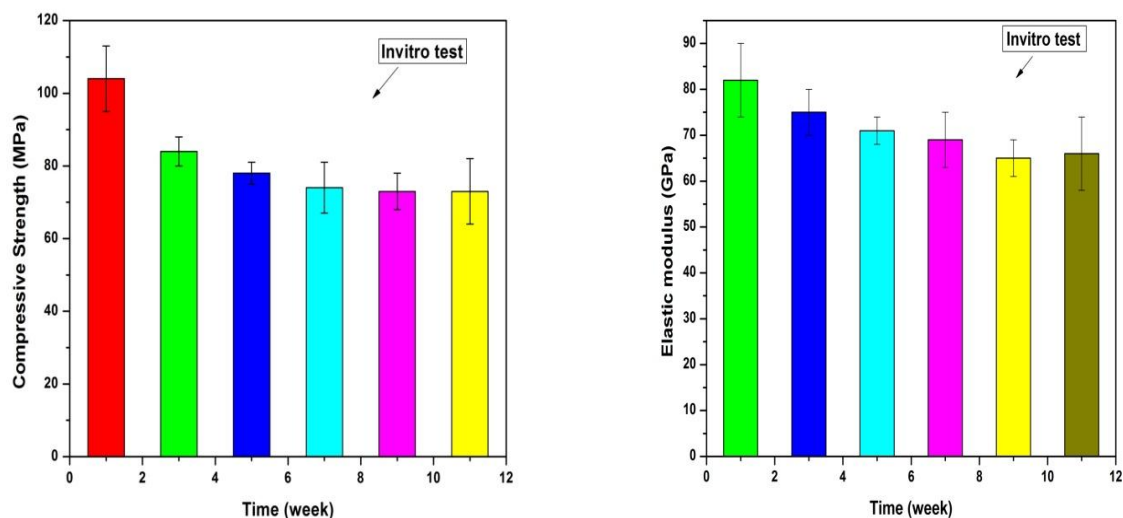

Fig.8 (a) Compressive strength and (b) elastic modulus as a function of time for HA and TiO2 reinforcement bioglass biocomposites after immersion in simulated body fluid (SBF) in vitro test.

3.3.3 Elastic properties of HA and TiO$_2$ reinforcement of biocomposites:-

The results indicate that the elastic moduli showed an anomalous with an initial addition of HA ,TiO2 and it increases with further addition of HA,TiO$_2$ content as shown in Fig.9. In BGHATi1 and BGHATi4 biocomposite, the measured young's and shear moduli ranges respectively from 47 to 82 GPa and 25 to 33 GPa. Similarly, the young's and bulk moduli ranges from 47 to 82 GPa and 33 to 53 GPa Fig.10 for BGHATi1 and BGHATi4

biocomposites. The increase in elastic moduli is due to an increase in the rigidity of bioglasses and TiO_2 content (A. V. Gayathri Devi et al.,2006).
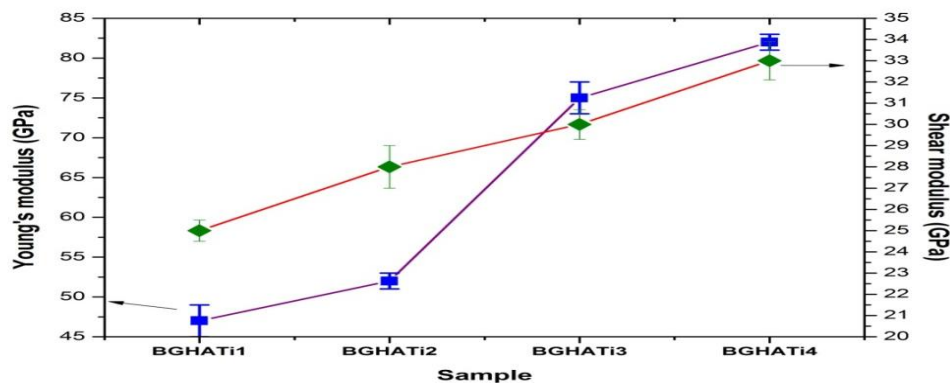

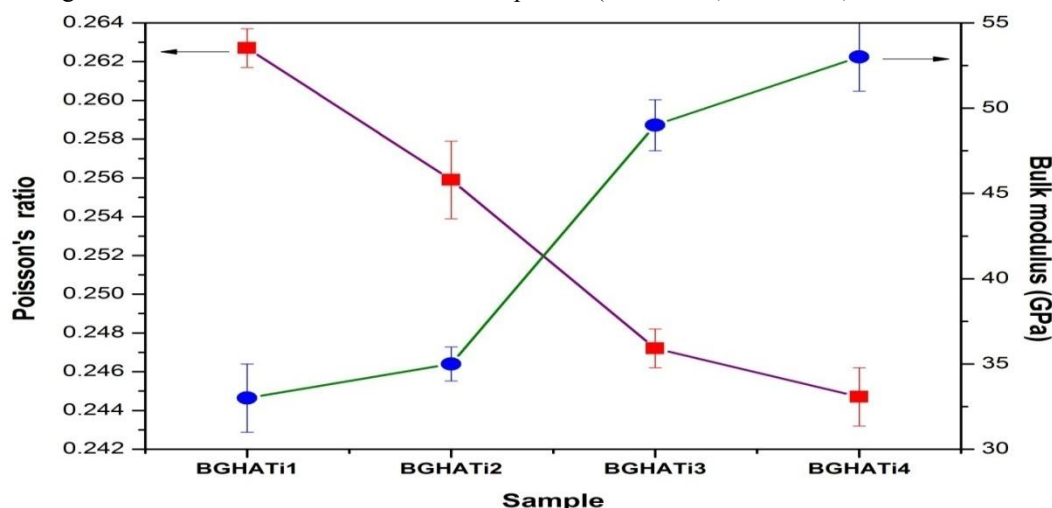Fig.9. Young's modulus and shear modulus of biocomposites (BGHATi1, BGHATi2, BGHATi3, BGHATi4).

Fig.10. Bulk modulus and poisson's'ratio of biocomposites (BGHATi1, BGHATi2, BGHATi3, BGHATi4).

Conclusion:-

Biocomposites with addition of HA and TiO_2 in Bioactive glass (45S5) are prepared respectively using sintering process. The presence of TiO_2 in silicate based 45S5 bioactive glass network results in higher rigidity which is explored from the observed increase in glass density. Due to the higher bonding ability of TiO_2, its results an increase in ultrasonic velocity. The elastic constants results support the above observation. The thermal treatment of silicate based glasses results in the release of stresses from the glass and the possible formation of crystalline phases along with the residual glassy phases.

Ti^{2+} ion was introduced in the glass composition for Si^{4+} ion in different concentrations (0-20 wt%) to yield a non charge valence series of bioglass based biocomposites. The increase of HA and TiO_2 content in bioglass composites result in increase of density, compressive strength, youngs, shear and bulk modulus while the poisson's ratio remained nearly constant. Mechanical property of the samples can be measured without any destruction of the biocomposites, since the biomaterials are very expensive to prepare.

Acknowledgment:-

Reference:-

1. **A. Agarwal and M. Tomozawa (1997).** Correlation of silica glass properties with the infrared spectra", Journal of Non - Crystalline Solids, vol. 209, pp. 166 - 174.
2. **A. Huygh, E. Schepers, L. Barbier, P. Ducheyne (2002).** Microchemical transformation of bioactive glass particles of narrow size range, a 0–24 months study, J. Mater. Sci. Mater. Med. 13: 315–320.
3. **A. J. Salinas, A.I. Martin, M. Vallet-Regi (2002).** Bioactivity of three CaO–P2O5–SiO2 sol–gel glasses, J. Biomed. Mater. Res. 61: 524–532.
4. **Albrektsson T, Hansson HA. (1986).** An ultrastructural characterization of the interface between bone and sputtered titanium or stainless steel surfaces. Biomaterials 7:201–5.
5. **A.V. Gayathri Devi, V. Rajendran, K. Jeyasubramanian, N. Suresh Kumar and S.A.M. Abdel-Hameed.(2006).** Ultrasonic Investigation on Nanocrystalline Barium Borate (BBO) Glass Ceramics, Synthesis and Reactivity in Inorganic, Metal-Organic and Nano-Metal Chemistry 36: 215-219.
6. **C.Q. Ning, Y. ZHOU, H. L. WANG, D. C. JIA, T. C. LEI (2000).** Apatite formation on the surface of a Ti/HA composite in a simulated body fluid, *J. Mater. Sci. Letters* 19 :1243–1245.
7. **C.Sarmento, Z.B. Luklinska, L. Brown, M. Anseau, P.N. De Aza, S. De Aza, F.J. Hughes I.J. McKay(2004**). In vitro behavior of osteoblastic cells cultured in the presence of pseudowollastonite ceramic, J. Biomed. Mater. Res. 69A :351–358.
8. **De Groot K, Klein CPAT, Wolke JGC, De Blieck-Hogervorst JMA. Chemistry of calcium phosphate bioceramics. In: Yamamuro T, Hench LL, Wilson J, editors (1990).** Handbook of bioactive ceramics, vol. II. Boca Raton, FL: CRC Press, p. 3–16.
9. **Delia S. Brauer, Natalia Karpukhina,Matthew D. O'Donnell,Robert V. Law, Robert G. Hill (2010).** Fluoride-containing bioactive glasses: Effect of glass design and structure on degradation, pH and apatite formation in simulated body fluid. Acta Biomaterialia 6 : 3275-3282.
10. **E. Schepers, M. De Clercq, P. Ducheyne, R. Kempeneers (1991).** Bioactive glass particulate material as a filler for bone lesions, J. Oral Rehabil. 18 : 439–452.
11. **Ebaretonbofa E and Evans. J G J. (2002).** Porous mater:257-9.
12. **Elliott JC, Mackie PE, Young RA. (1973).** Monoclinic hydroxyapatite. Science :180:1055–7.
13. **E.M.A. Khalil, F.H. ElBatal, Y.M. Hamdy, H.M. Zidan, M.S. Aziz and A.M. Abdelghany (2010).** Infrared absorption spectra of transition metals - doped soda lime silica glasses",Physica B, vol. 405, pp. 1294 - 1300.
14. **F. Moztarzadeh (1988).** Electrical conductivity of Y_2O_3 stabilized zirconia, Ceram. Int. 14: 27–30.
15. **Hench LL, Wilson J.(1984).** Surface-active biomaterials. Science :226:630–6.
16. **Hench LL. (1998).** Bioceramics. J Am Ceram Soc:81:1705–28.
17. **Himanshu Tripathi, Sumit Kumar Hira, Arepalli Sampath Kumar, Uttam Gupta, Partha Pratim Manna, S.P. Singh (2015).** Structural characterization and in vitro bioactivity assessment of SiO_2–CaO–P_2O_5–K_2O–Al_2O_3 glass as bioactive ceramic material, *Ceramics International* 41:11756–11769.
18. **J. Wang, W. Suna, Z. Zhang, Z. Jianga, X. Wang, R. Xu, R. Li, X. Zhang (2008).** J. Colloid Interface Sci.320: 202.
19. **Jarcho M. (1981).** Calcium phosphate ceramics as hard tissue prosthetics. Clin Orthop Relat Res:157:259–78.
20. **Julian R. Jones (2013).** Review of bioactive glass: from Hench to hybrids, Acta Biomater. 9 : 4457–4486.
21. **K. DE Groot (1980).** *Biomater.* 1 :47.
22. **K P Santosh,Min-Cheol Chu,A Balakrishnan,T N Kim and Seong-Jai Cho.(2009).** Preparation and characterization of nano-hydroxyapatite powder using sol-gel technique. Bull Mater. Sci.:Vol.32 No.5:465-470.
23. **Kokubo T, Takadama H (2006).** Biomaterials; 27:2907–15.
24. **L.L. Hench (2006).** The story of bioglass, J. Mater. Sci. Mater. Med 17: 967–978.

25. **L.L. Hench, R.J. Splinter, W.C. Allen, T.K. Greenlee (1971).** Bonding mechanisms at the interface of ceramic prosthetic materials, J. Biomed. Mater. Res. 334 :117–141.
26. **L.L. Hench, J.M. Polak (2002).** Third-generation biomedical materials, Science 295 :1014–1017.
27. **Long M, Rack HJ. (1998).** Titanium alloys in total joint replacement-a materials science perspective. Biomaterials19:1621–39.
28. **Lutz-Christian Gerhardt 1 and Aldo R. Boccaccini 1,2 (2010).** Bioactive Glass and Glass-Ceramic Scaffolds for Bone Tissue Engineering, Materials 3:3867-3910.
29. **M.A. Lopes, J.D. Santos, F.J. Monteiro, J.C. Knowles (1998).** Glass-reinforced hydroxyapatite: a comprehensive study of the effect of glass composition on the crystallography of the composite, J. Biomed. Mater. Res. 39 :244–251.
30. **Marta Cerrutia, David Greenspanb, Kevin Powers (2005).** Biomaterials 26 :1665–1674.

31. **Nanci A, Wuest JD, Peru L, Brunet P, Sharma V, Zalzal S, McKee MD (1998).** Chemical modification of titanium surfaces for covalent attachment of biological molecules. J Biomed Mater Res 40:324–35.
32. **P.N. De Aza, J.M. Ferna´ndez-Pradas, P. Serra (2004).** In vitro bioactivity of laser ablation pseudowollastonite coating, Biomaterials 25:1983–1990.
33. **P.N. De Aza, Z.B. Luklinska, Martinez, M.R. Anseau, F. Guitian, S. De Aza (2000).** Morphological and structural study of pseudowollastonite implants in bone, J. Microsc. 197 :60–67.
34. **P.N. De Aza, Z.B. Luklinska, M.R. Anseau, F. Guitian, S. De Aza (1999).** Bioactivity of pseudowollastonite in human saliva, J. Dent. 27 :107–113.
35. **Ruys AJ, Brandwood A, Milthorpe BK, Dickson MR, Zeigler KA, Sorrell CC. (1995).** The effect of sintering atmosphere on the chemical compatibility of hydroxyapatite and particulate additives at 12001C. J Mater Sci: Mater Med 6:297–301.
36. **X. Sun, H. Liu, J. Dong, J. Wei, Y. Zhang (2010).** Catal. Lett., 135 :219.